

EVALUATING THE EFFECTS OF NITROGEN DOPING AND OXYGEN DOPING ON SRF CAVITY PERFORMANCE*

H. Hu[†], Y.-K. Kim, University of Chicago, Chicago, IL, USA
D. Bafia, Fermi National Accelerator Laboratory, Batavia, IL, USA

Abstract

Superconducting radiofrequency (SRF) cavities are resonators with extremely low surface resistance that enable accelerating cavities to have extremely high quality factors (Q_0). High Q_0 decreases the capital required to keep the accelerators cold by reducing power loss. The performance of SRF cavities is largely governed by the surface composition of the first 100 nm of the cavity surface. Impurities such as oxygen and nitrogen have been observed to yield high Q_0 , but their precise roles are still being studied. Here, we compare the performance of cavities doped with nitrogen and oxygen in terms of surface composition and heating behavior with field. A simulation of the diffusion of oxygen into the bulk of the cavity was built using COMSOL Multiphysics software. Simulated results were compared to the actual surface composition of the cavities as determined from secondary ion mass spectrometry analysis. Understanding how these impurities affects performance allows us to have further insight into the underlying mechanisms that enable these surface treatments to yield high Q_0 .

INTRODUCTION

The role of impurities in Nb is critical in SRF cavity performance. Nitrogen doped cavities have displayed high quality factors (Q_0) of $> 4 \times 10^{10}$ and high accelerating gradients (E_{acc}) of > 38 MV/m [1]. Recent work has shown that low temperature baking (LTB), which relies on diffusion of oxygen from the native oxide, mitigates high field Q-slope (HFQS) and improves Q_0 at high E_{acc} [2]. Motivated by these studies on LTB, we conduct initial studies on a new treatment technique called oxygen doping, also referred to as oxygen alloying, which achieves doping-like performance but without any extrinsic impurities [3]. Oxygen doping diffuses oxygen from the native oxide following Fick's second law to achieve a uniform concentration of impurities in the first 100 nm of the surface [3]. Solutions to this diffusion process have been analytically obtained in Refs. [4, 5]. We take an alternative approach by simulating the diffusion process of oxygen into niobium. With this simulation, we can associate cavity performance with an impurity profile such that the oxygen doping treatment can be fine tuned for the desired performance.

This work presents an initial study evaluating and understanding the precise roles of oxygen and nitrogen in enabling

high Q_0 . We find that even in the absence of nitrogen, we can achieve doped-like anti-Q slope performance, as well as high Q_0 and E_{acc} . The biggest discrepancy seems to lie in the turning on of additional loss mechanisms at higher fields, driving both higher resistance as well as causing significant heating within the cavity. Further work is required to optimize this treatment and understand the causes of these high field losses. Initial data supports that oxygen doping a promising treatment comparable to nitrogen doping.

EXPERIMENTAL METHOD

One single cell, TESLA shaped Nb cavity with resonant frequency of 1.3 GHz was first baselined with an 800°C degas and 40 μm electropolishing (EP) removal [2]. The cavity was then treated with subsequent steps of baking and chemical processing. First, the cavity was *in-situ* baked at 200°C to diffuse oxygen from the native niobium oxide into the bulk. Next, the cavity underwent two rounds of HF rinsing to strip the oxide, leaving the Nb metal untouched. Following each HF rinse, the cavity was exposed to air to allow a new, undepleted Nb_2O_5 layer to form [6]. The regrowth process consumes about 2 μm of Nb but otherwise, the impurity profile of the rf layer is unaffected [6]. After each treatment, the cavity was tested to find Q_0 vs. E_{acc} at both 2 K and low T (< 1.5 K) in continuous wave (CW) operation to determine the decomposition of surface resistance into BCS and residual resistances [7]. Before testing, the cavity was evacuated and assembled with resistance temperature detectors (RTDs), flux gates at the equator, and Helmholtz coils. The cavity was cooled to 4.2 K with the fast cool down protocol to minimize the possibility of trapping magnetic flux [2].

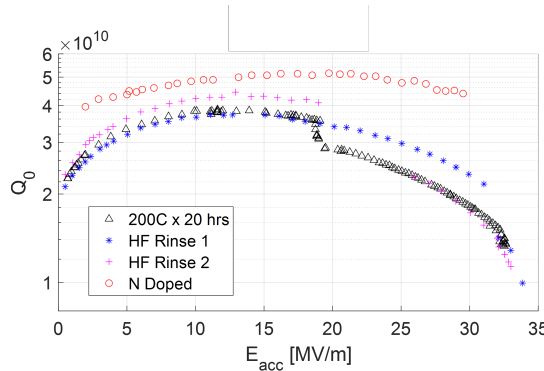
In addition to Q_0 and E_{acc} , we also investigated how the cavity heated with increasing fields using thermometry mapping (TMAP) [8]. 576 carbon RTDs were installed on the outside of the cavity during assembly. The temperature at each RTD was recorded periodically during CW testing. In parallel with cavity testing, we also treated cavity cutouts of 1 cm in diameter to the same treatments as the single cell cavity. These samples were analyzed with time of flight secondary ion mass spectrometry (TOF-SIMS) to associate performance with surface composition [9].

RESULTS AND DISCUSSION

We compare the performance for each of our three treatment steps with that of a nitrogen doped single cell cavity that was treated with 2/0 + 5 μm EP nitrogen doping [1]. Data for the nitrogen doped cavity is from Ref. [8].

* Work supported by the Fermi National Accelerator Laboratory, managed and operated by Fermi Research Alliance, LLC under Contract No. DE-AC02-07CH11359 with the U.S. Department of Energy; the University of Chicago.

[†] hannahhu@uchicago.edu

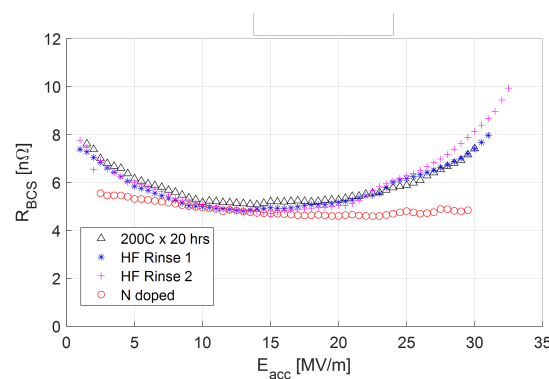
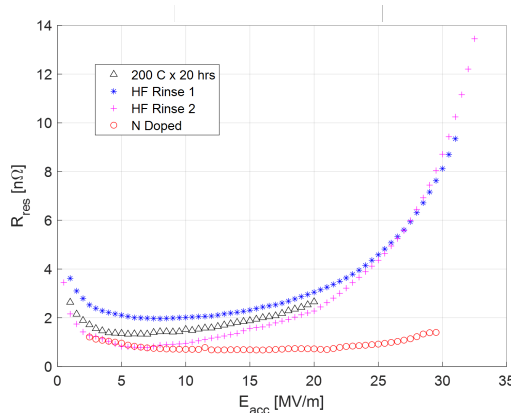
Figure 1: Q_0 vs. E_{acc} data taken at 2 K acquired at Fermilab VTS system.

Q_0 vs E_{acc}

Figure 1 plots the behavior of Q_0 vs E_{acc} at 2 K. During the $200^\circ\text{C} \times 20$ hr test, the cavity experienced an initial quench at around 19 MV/m from field emissions. This trapped magnetic flux and decreased Q_0 . The test after HF rinse 2 experienced a quench due to multipacting at 20 MV/m, which prevented data from being taken until 25 MV/m and also trapped flux. All three tests had final quenches around 33–34 MV/m. Although the peak quality factor of about 4.2×10^{10} is not as high as that of a nitrogen doped cavity, it is still excellent performance. In addition, we observe a phenomenon known as the anti-Q slope that is characteristic of nitrogen doped cavities in which Q_0 increases with E_{acc} . This displays the potential of oxygen doping as a treatment capable of achieving high performance comparable to nitrogen doping.

BCS Resistance

BCS surface resistance (R_{BCS}) is shown Fig. 2. R_{BCS} is very similar for all three tests. The initial decrease in BCS resistance with accelerating gradient is what drives the anti-Q slope phenomenon [1]. The similarities in the BCS resistance, despite the additional HF rinses, suggests that the differences in Q_0 vs E_{acc} are not driven by impurities in the rf layer. Compared to that of a nitrogen doped cavity, we

Figure 2: R_{BCS} vs. E_{acc} data showing the temperature dependent component of resistance at 2 K.Figure 3: R_{res} vs. E_{acc} data of the temperature independent resistance without trapped flux contribution.

see that minimum R_{BCS} is about the same, but at high fields, oxygen doped cavity has significantly higher R_{BCS} . This indicates there are additional sources of loss for the oxygen doped cavity that are not present in the nitrogen doped one that are turned on at higher fields.

Residual Resistance

The temperature independent residual resistance (R_{res}) is displayed in Fig. 3. Any contribution from trapped magnetic flux has been subtracted from the data shown. We see that after the $200^\circ\text{C} \times 20$ hr *in-situ* bake, the R_{res} is moderately low. After the first HF rinse, we expected R_{res} to decrease, but observed a counter-intuitive increase instead, suggesting that the depleted oxide was not completely refreshed, as the suboxides that grow during baking are metallic and weaken the overall superconductivity. Thus, the cavity was HF rinsed a second time. After the second HF rinse, R_{res} decreased as expected. Regrowing the native oxide appeared to mitigate some of the sources of loss, indicating that the growth of suboxides from *in-situ* baking may have driven lower Q_0 . Compared to the nitrogen doped R_{res} , we observe a similar minimum value, but again, the resistances are significantly higher for the oxygen doped cavity at higher accelerating gradients. For the rest of this paper, we will solely consider data from the cavity after the second HF rinse since we believe that we have a full undepleted native oxide to enable better comparison with a nitrogen doped cavity.

TMAP and Heating Profile

Figure 4 is a temperature map of the entire cavity just before a quench occurs. The color scale is logarithmic with the actual temperature of each sensor displayed in mK. There is minimal heating in the cavity except at the equator, where at the point of highest heating (also the location of initial quench), the temperature change is 390 mK.

The heating profile for a particular sensor is acquired by recording the change in temperature as a function of peak magnetic field for each TMAP. Figure 5 shows the heating profile at the quench location. This heating profile is compared to that of a nitrogen doped cavity which also quenched

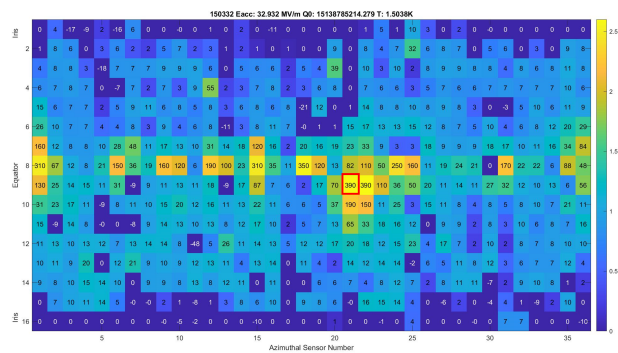


Figure 4: Map of the temperature within the cavity at quench. Quench location is labeled in red.

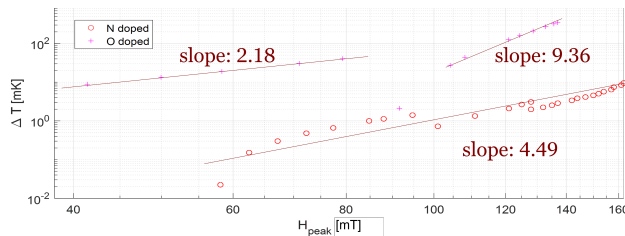


Figure 5: Heating profile at the location of quench.

near the equator. On a log-log scale, if the change in temperature is due to pure joule heating, we would expect there to be a slope of 2 according to Ohm's law. At low fields, the slope is 2.18, but there is a sudden discontinuous change to 9.36. The drop in temperature at $H_{peak} \approx 80$ mT is a result of the cavity losing resonance due to multipacting. In the 10 minutes it took to recover resonance, the cavity had cooled down significantly. The discontinuity in slope suggests the turning on of additional loss mechanisms, leading to a temperature change that is 40 times greater than what is observed in a nitrogen doped cavity. The exact loss mechanisms that turned on at higher fields are still under investigation.

COMSOL

Figure 6 shows the data from SIMS of oxygen concentration as a function of depth [9]. The data displays the change in the surface composition after 3, 19, and 45 hr of baking at 205° C. Data for the normalized surface composition is from Ref. [9]; the signal of O^-/Nb^- is normalized for ease of comparison with simulated results. We built a simplified simulation in COMSOL Multiphysics using the transport of diluted species (tds) interface of the 1-dimensional diffusion of oxygen from the surface into the niobium bulk. We assumed that the initial concentration of oxygen was constant and that the niobium did not have any oxygen impurities initially. Figure 6 also contains the simulated curves at these three times, and the simulated results have good agreement with the collected SIMS data. Further work involves developing the simulation for the diffusion of oxygen into a non-pure bulk.

MC7: Accelerator Technology

T07: Superconducting RF

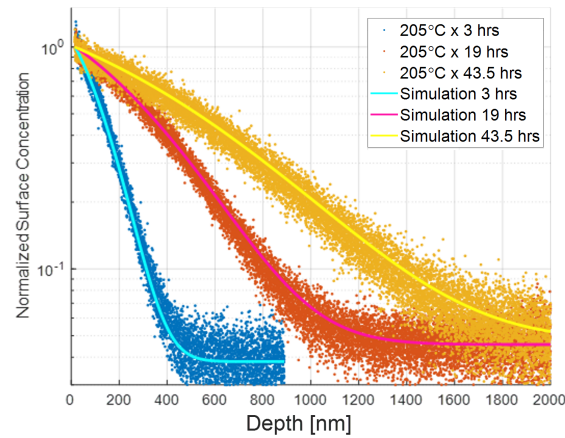


Figure 6: SIMS data showing impurity profiles for three different baking times (data from Ref. [9]) and simulation results from COMSOL.

CONCLUSION

We observed that oxygen doping and nitrogen doping treatments yield similar rf performance. From the residual resistance, we see that eliminating suboxides and regrowing the native oxide led to an increase in quality factor. For both residual and BCS resistance, the oxygen doped cavity had much higher resistance at higher accelerating gradients compared to that of a nitrogen doped cavity. The heating profile acquired from TMAP data confirmed this since there is substantial heating in the oxygen doped cavity that is not present in the nitrogen doped one that could possibly be from the loss mechanism turning on at higher fields. Overall, more studies are required to delineate the role that oxygen is playing in SRF cavity performance. Oxygen doping seems to be a viable replacement for nitrogen doping, but more tests are needed to assess the robustness of this treatment. A complete sweep of the oxygen doping parameter space may reveal unprecedented performance for cavities which could enable the next generation of accelerators.

REFERENCES

- [1] A. Grassellino *et al.*, "Nitrogen and argon doping of niobium for superconducting radio frequency cavities: a pathway to highly efficient accelerating structures", *Supercond. Sci. Tech.*, vol. 26, pp. 102001, 2013. doi:10.1088/0953-2048/26/10/102001
- [2] D. Bafia *et al.*, "The role of oxygen concentration in niobium SRF cavities", in *Proc. SRF'21*, Lansing, MI, Jun. 2021, paper THPTEV016, unpublished.
- [3] D. Bafia *et al.*, "Investigating the anomalous frequency variations near T_c of Nb SRF cavities", in *Proc. SRF'21*, Lansing, MI, Jun. 2021, paper FROFDV03, unpublished.
- [4] E. M. Lechner *et al.*, "RF surface resistance tuning of superconducting niobium via thermal diffusion of native oxide", *Appl. Phys. Lett.*, vol. 119, pp. 082601, 2021. doi:10.1063/5.0059464
- [5] S. Calatroni *et al.*, "Diffusion of Oxygen in Niobium during Bake-out", in *Proc. SRF'01*, Tsukuba, Japan, Sep. 2001.

- [6] A. Romanenko *et al.*, “Effect of mild baking on superconducting niobium cavities investigated by sequential nanoremoval”, *Phys. Rev. ST Accel. Beams* vol. 16, pp. 012001, 2013. doi:10.1103/PhysRevSTAB.16.012001
- [7] M. Martinello *et al.*, “Effect of interstitial impurities on the field dependent microwave surface resistance of niobium”, *Appl. Phys. Lett.* vol. 109, pp. 062601, 2016. doi:10.1063/1.4960801
- [8] D. Bafia, “Exploring and Understand the Limitations of Nb SRF Cavity Performance”, Ph.D. thesis, Phys. Dept., Illinois Institute of Technology, Chicago, IL, 2020.
- [9] A. S. Romanenko *et al.*, “First Direct Imaging and Profiling TOF-SIMS Studies on Cutouts from Cavities Prepared by State-of-the-Art Treatments”, in *Proc. SRF’19*, Dresden, Germany, Jun.-Jul. 2019, pp. 866-870. doi:10.18429/JACoW-SRF2019-THP014